ELSEVIER

Synthesis and reactivity of heterometallic RhO–M (M = Si, Ti) complexes Memory effect in their catalytic performance in CO hydrogenation

M. Ojeda [a], R. Fandos [b,1], J.L.G. Fierro [a], A. Otero [c], C. Pastor [e],
A. Rodríguez [d], M.J. Ruiz [b], P. Terreros [a,*]

[a] *Instituto de Catálisis y Petroleoquímica, CSIC, C/Marie Curie 2, 28049 Madrid, Spain*
[b] *Facultad de Ciencias del Medio Ambiente, UCLM, Avda. de Carlos III, s/n, 45061 Toledo, Spain*
[c] *Facultad de Ciencias Químicas, UCLM, Campus Ciudad Real, 13071 Ciudad Real, Spain*
[d] *ETS Ingenieros Industriales, UCLM, Campus Ciudad Real, 13071 Ciudad Real, Spain*
[e] *Servicio Interdepartamental de Apoyo a la Investigación, Facultad de Ciencias, Universidad Autónoma de Madrid, Madrid, Spain*

Abstract

The titanium salycilate complex [Cp*Ti(sal)(salH)] **1** (salH$_2$ = salycilic acid) was synthesised by reacting Cp*TiMe$_3$ and salycilic acid. The molecular structure of **1** studied by X-ray shows it to be dinuclear with a carboxylate group acting as a bridge ligand. [Rh(μ-OH)COD]$_2$ reacts with **1** to yield the bimetallic complex **2**, or with the siloxanodiol (HOSiPh)$_2$O to yield the bimetalic bis-siloxide Rh complex **3**. Carbon monoxide displaces COD in **2** and **3** to give the carbonylic complexes **4** and **5** respectively. Complex **4** can also be prepared from **2** and [Rh(acac)(CO)$_2$]. Compounds **2**, **3**, **4** and **5** can be envisaged as models of Rh complexes anchored on titania or silica. The catalytic performance of heterometallic complexes is studied in the CO hydrogenation reaction and compared to rhodium-based (Rh-based) catalysts prepared by impregnation from Rh(NO$_3$)$_3$ or [Rh(acac)(CO)$_2$] showing higher yields to oxygenated products.
© 2005 Elsevier B.V. All rights reserved.

Keywords: Early–late heterometallic complexes; CO hydrogenation; Rhodium; O ligands; Titanium; Silicon

1. Introduction

The chemistry of heteronuclear complexes has been extensively studied due to its importance in different areas. Those compounds containing an oxygen atom as bridging ligand between the noble metal and the other component can be envisaged as models of noble metals deposited on inorganic oxides (SiO$_2$, TiO$_2$, etc.). Knowing in detail, at molecular level, the properties of the active centre is of a great importance. The oxide used as support is also a key feature in this interaction. When titania or other reducible oxides are used, the phenomenon known as strong metal support interaction (SMSI) can be produced when the H$_2$ reduction is carried out at high temperature ($\geq$773 K). The catalytic performance is then severely affected [1].

The nature of the metal-support interaction can be modulated by many factors, i.e., the preparation method, metal precursor and the transition metal compounds used in the catalyst preparation [2,3]. The ligands in the coordination sphere plus the interaction with the support will account for the nature of the metal grafted species.

In this sense, we have carried on with the study of transition-metal alkoxides [4] to other O containing ligands.

We report here the synthesis of a salicylate titanium compound and we study its reactivity with [Rh(μ-OH)(COD)]$_2$ which leads to the formation of the corresponding early–late heterometallic complex that can be considered as molecular model for a late metal catalysts supported on titania. On the other hand, we report the synthesis and characterization of a Rh (I) siloxide complex that constitute a good model for rhodium complexes supported on a silica surface.

* Corresponding author. Tel.: +34 915854768; fax: +34 915854760.
  E-mail addresses: rfandos@amb-to.uclm.es (R. Fandos),
pterreros@icp.csic.es (P. Terreros).
  [1] Tel.: +34 925265727; fax: +34 925268841.

Besides, we have studied their reactivity towards CO and the catalytic behaviour in the CO hydrogenation (Fischer–Tropsch synthesis). The interest of this reaction has continuously grown up in the last years as demonstrated by some reviews published recently [5–7]. The synthesis of hydrocarbons from CO hydrogenation over transition metals is perhaps the most promising source of chemicals and fuels from non-petroleum-based supply such as coal and natural gas. The reaction selectivity depends strongly on the metal used as a catalyst. When Fe and/or Co is used, the reaction products consist in a mixture of paraffins and olefins, while oxygenates compounds are obtained with rhodium-based catalysts. In this work, we compare the catalytic performance of conventional Rh-based catalysts prepared from the usual precursors (rhodium chloride and nitrate) or closely related complexes ([Rh(acac)(CO)$_2$]), with that corresponding to the Rh complexes used as models. The nature of the active centre plus the support interaction in the big scale FT reaction is of a great importance to modulate the selectivity towards the desired products [8,9].

2. Experimental

2.1. General procedures

The preparation and handling of the described compounds was performed with rigorous exclusion of air and moisture under nitrogen atmosphere using standard vacuum line and Schlenk techniques. All solvents were dried and distilled under a nitrogen atmosphere.

The following reagents were prepared according to literature procedures: [TiCp*(Me)$_3$] [10], [Rh(μ-OH)(COD)]$_2$ [11,12], and Cp*Ti(O$_2$Bz)$_2$Rh(COD) [4].

The commercially available compounds, salicylic acid and LiMe in diethyl ether were used as received from Aldrich.

^{1}H and ^{13}C NMR spectra were recorded on a 200 Mercury Varian Fourier Transform spectrometer. Trace amounts of protonated solvents were used as references, and chemical shifts are reported in units of parts per million (ppm) relative to SiMe$_4$.

Transmission infrared spectra were obtained on a Nicolet ZDX Fourier transform IR spectrophotometer connected to a Nicolet 680 Spectral Workstation equipped with a DTGS detector.

Thermal analyses of the fresh catalysts were performed on a Mettler Toledo TGA/SDTA 851 apparatus. Typically, about 10 mg of the sample was heated from 298 to 1223 K at a rate of 1 K/min under H$_2$ flow.

2.2. Preparation of compounds

2.2.1. [TiCp*(sal)(salH)] (1)

To a solution of [TiCp*(Me)$_3$] (0.234 g, 1.03 mmol) in 5 mL of toluene, at 233 K, was added salicylic acid (0.283 g, 2.05 mmol). The mixture was allowed to reach the room temperature and then was stirred for 1 h. After filtration, the solvent was removed under vacuum and the residue washed with 5 mL of pentane to yield complex 1 as a dark red solid. Yield: 0.357 g, 76%. IR (KBr, cm^{-1}): 1603 (vs), 1570 (s), 1530 (s), 1457 (vs),

1399 (m), 1380 (m), 1317 (w), 1247 (m), 1142 (w), 1030 (w), 879 (w), 825 (w), 762 (m), 704 (w), 669 (w). ^{1}H NMR (CDCl$_3$, rt, 200 MHz): 1.87 (s, 15 H, Cp*), 2.11 (s, 15 H, Cp*), 6.48–8.5 (m, 16 H, Ar), 10.19 (br, 1 H, OH), 12.8 (br, 1 H, OH). ^{13}C{^{1}H} NMR: 12,5 (s, Cp*), 13,4 (s, Cp*), 114.3 (s, Ar$_{ipso}$), 114.8 (s, Ar$_{ipso}$), 116.2 (s, Ar$_{ipso}$). 119.5 (s, Cp*), 117.7, 118.5, 119.2, 119.6, 120.6, 120.7, 131.0, 131.1, 131.9, 131.9, 132.4, 134.6, 135.3, 135.5, 135.7, 135.8 (s, Ar), 161.7, 167.4, 168.1, 170.9 (s, Ar$_{ipso}$), 174.3, 174.6, 175.5, 182.4 (s, COO). Anal. Cald. for C$_{24}$H$_{24}$O$_6$Ti: C, 63.17; H, 5.30. Found: C, 63.66; H, 5.51.

2.2.2. [TiCp*(sal)$_2$Rh(COD)] (2)

To a solution of complex 1 in CH$_2$Cl$_2$ (0.142 g, 0.31 mmol) was added [Rh(μ-OH)(COD)]$_2$ (0.071 g, 0.15 mmol) and the mixture was stirred at room temperature for 30 min. After that, the solvent was removed under vacuum and the residue washed with pentane to yield an orange solid, which was characterized as complex 2 (0.134 g, 65%). IR (KBr, cm^{-1}): 1598 (s), 1567 (s), 1516 (vs), 1457 (vs), 1382 (m), 1315 (w), 1247 (m), 1141 (m), 1029 (w), 893 (m), 833 (m), 754 (m), 701 (w), 676 (w), 636 (w), 596 (w). ^{1}H NMR (CD$_2$Cl$_2$, rt, 200 MHz): 1.66 (m, 4 H, COD), 2.12 (s, 15 H, Cp*), 2.40 (m, 4 H, COD), 4.10 (m, 4 H, COD), 6.78 (m, 2 H, Ar), 6.84 (m, 2 H, Ar), 7.39 (m, 2 H, Ar), 7.84 (m, 2 H, Ar). ^{13}C{^{1}H} NMR: 12,2 (s, Cp*), 31,0 (s, COD), 77.7 (br, COD), 119.2, 120.1, 132.3, 134.9 (s, Ar), 131.6 (s, Cp*), 166.7 (s, Ar$_{ipso}$), 172.8 (s, COO). Anal. Cald. for C$_{32}$H$_{35}$O$_6$TiRh: C, 57.67; H, 5.29. Found: C, 57.58; H, 5.53.

2.2.3. [{Rh(COD)}$_2${μ-(OSiPh$_2$)$_2$O}] (3)

To mixture of [Rh((-OH)(COD)]$_2$ (0.090 g, 0.20 mmol) and (HOSiPh$_2$)$_2$O (0.082 g, 20 mmol) was added toluene (8 mL) at room temperature and the solution was stirred for 1 h. After that, the solvent was partially evaporated under vacuum. Slow diffusion of pentane into the toluene solution afforded yellow crystals of 3. (0.101 g, 61%). IR (KBr, cm^{-1}): 1428 (m), 1115 (s), 1001 (m), 977 (vs), 964 (s), 914 (s), 871 (m), 743 (w), 713 (s), 699 (s), 527 (vs). ^{1}H NMR (C$_6$D$_6$, rt, 200 MHz): 1.24 (m, 4 H, COD), 1.58 (m, 4 H, COD), 1.83 (m, 4 H, COD), 2.57 (m, 4 H, COD), 3.59 (m, 4 H, COD), 4.34 (m, 4 H, COD), 7.20 (m, 12 H, Ar), 8.13 (m, 8 H, Ar). ^{13}C{^{1}H} NMR: 30,7 (s, COD), 31,2 (s, COD), 76.5 (d, J = 14.5 Hz, COD), 77.7 (d, J = 14.5 Hz, COD), 127.8, 129.7, 135.3 (s, Ar), 138.9 (s, Ar$_{ipso}$). Anal. Cald. for C$_{40}$H$_{44}$O$_3$Si$_2$Rh$_2$: C, 57.55; H, 5.31. Found: C, 57.72; H, 5.09.

2.2.4. [TiCp*(sal)$_2$(Rh(CO)$_2$)] (4)

CO was bubbled through a suspension of 2 in hexane for 30 min in an ice bath. The red solid was filtered off and washed with cold hexane. Yield: 80%. IR (KBr, cm^{-1}): 2083 (vs), 2008 (vs), 1600 (s), 1567 (s), 1497 (vs), 1457 (vs), 1391 (m), 1316 (w), 1246 (m), 1142 (w), 1029 (w), 895 (m), 835 (m), 757 (m), 702 (w), 677 (w), 635 (w), 604 (w); Anal. Cald. for C$_{26}$H$_{23}$O$_8$TiRh: C, 50.75; H, 3.77. Found: C, 51.35; H, 3.89.

2.2.5. [{Rh(CO)$_2$}$_2${μ-(OSiPh$_2$)$_2$O}] (5)

CO was bubbled through a suspension of 3 in hexane for 20 min in an ice bath. The yellow pale solid was filtered off and washed with hexane. Yield: 82%. IR (KBr, cm^{-1}): 2077 (vs),

2017 (vs), 1429 (w), 1116 (s), 1091 (s), 919 (s), 964 (s), 741 (w), 718 (m), 698 (s), 568 (m), 529 (m). ^{1}H NMR (C$_6$D$_6$, rt, 200 MHz): 7.23 (m, 12 H, Ar), 8.10 (m, 8 H, Ar). ^{13}C{^{1}H} NMR: 128.1, 130.7, 135.7 (s, Ar), 136.0 (s, Ar$_{ipso}$), 180.8 (d, $^1J_{Rh-C} = 74.7$ Hz, CO). Anal. Cald. for C$_{28}$H$_{20}$O$_7$Si$_2$Rh$_2$: C, 46.04; H, 2.76. Found: C, 46.37; H, 3.19.

2.3. Catalysts preparation

The Rh/γ-Al$_2$O$_3$ sample (reference) containing 3 wt.% of Rh was prepared by impregnation of γ-Al$_2$O$_3$ (Condea Puralox Nwa–155, $S_{BET} = 150$ m^2/g) with an aqueous solution of Rh(NO$_3$)$_3$·xH$_2$O). Samples **7** and **8** were prepared by using the same support but [Rh(acac)(CO)$_2$] as metal precursor. For the preparation of samples named as **9** and **10**, silica (PQ Corporation, MS-3030, $S_{BET} = 300$ m^2/g) was used as a support and [Rh(acac)(CO)$_2$] as rhodium precursor. In all cases, the preparation procedure was similar, and the rhodium metal loading was ∼3 wt.%. The support and the impregnating solution were stirred for several hours and then, water was removed by controlled evaporation in a rotary evaporator. Following, the sample was dried at 383 K for 6 h and finally calcined at 773 K for 12 h in air. A detailed charaterisation study of these samples has been reported elsewhere [13,14].

2.4. Catalytic measurements

CO hydrogenation reactions were performed using a high-pressure fixed-bed microreactor (stainless steel 316, 150 mm length and 9 mm internal diameter). The samples (0.25–0.30 mm particle size) were directly diluted with SiC (0.25–0.30 mm particle size) to avoid hot spots. The weight of sample and SiC were changed for each experiment in order to keep constant the amount of Rh and the volume of the catalytic bed. In some experiments, the catalysts were previously reduced in situ at 533 K (heating rate of 10 K/min) for 1 h in a flow of H$_2$/N$_2$ (1:9) at a rate of 100 mL/min. The reactor was then cooled down and the gas flow was switched to 50 mL/min of syngas (molar ratio H$_2$/CO = 2). The system was pressurized at 2.03 MPa and the reactor temperature was increased at a heating ramp of 10 K/min. Temperature was measured with a type-K thermocouple buried in the catalytic bed. Flow rates were controlled using a Brooks 5850 TR Series mass flow controllers. All experimental variables were carefully controlled to ensure identical reaction conditions when testing catalysts. Once the catalyst reached the steady-state (about 3-4 h), the catalytic performance was measured for about 48 h, showing no deactivation and high catalytic stability.

Product analysis was performed on-line with a gas chromatograph (HP 5890 Series II) equipped with TCD and FID detectors and two in-series fused silica capillary columns: SPB-5 (60 m × 0.53 mm) and Supel-Q Plot (30 m × 0.53 mm). It was possible to analyze inorganic gases (H$_2$, CO and CO$_2$), C$_1$–C$_{20}$ hydrocarbons, C$_1$–C$_{10}$ alcohols, and other oxygenated compounds. The identification of reaction products and gas chromatograph calibration were accomplished using gas chromatography-mass spectrometry (GC–MS) and quantitative standard solutions from AccuStandard.

2.5. X-ray data collection

A red single crystal of approximate dimensions 0.15 × 0.10 × 0.04 mm with prismatic shape of **1** was mounted on a glass fibber and transferred to a Bruker SMART 6 K CCD area-detector three-circle diffractometer with a MAC Science Rotating Anode (Cu Kα radiation, λ = 1.54178 Å) generator equipped with Goebel mirrors at settings of 45 kV and 100 mA. X-ray data were collected at 100 K, with a combination of six runs at different φ and 2θ angles, 3600 frames. The data were collected using 0.3° wide ω scans (2 s/frame at 2θ = 40° and 6 s/frame at 2θ = 100°), crystal-to-detector distance of 5.0 cm.

The substantial redundancy in data allows empirical absorption corrections (SADABS) [15] to be applied using multiple measurements of symmetry-equivalent reflections. The software package SHELXTL [16–18] version 6.10 was used for space group determination, structure solution and refinement. The structure was solved by direct methods (SHELXS-97) [17], completed with difference Fourier syntheses, and refined with full-matrix least-squares using SHELXL-97 [18] minimizing $\omega(F_0^2 F_c^2)^2$. All non-hydrogen atoms were refined with anisotropic displacement parameters. The hydrogen atom positions were calculated geometrically and were allowed to ride on their parent carbon atoms with fixed isotropic U.

The compound has a molecule of solvent disordered that seems to be pentane. This disorder was impossible to model. In the solvent and in the empirical formula were not included the hydrogen atoms.

A single crystal of a yellow block of **3** was placed on a NONIUS-MACH3 diffractometer equipped with a graphite monochromated Mo Kα radiation (λ = 0.71073 Å). Intensity data were collected by using an ω/2θ scan technique. Examination of two standard reflections, monitored after 60 min, showed no signal of crystal deterioration. Data were corrected for Lorentz and polarization effects, and semi-empirical absorption correction (Psi-scans) was carried out [19]. The structures were solved by the direct methods using the SIR92 computer software [20], completed by subsequent difference Fourier syntheses, and refined by full matrix least-squares procedures (SHELXL97) [18] on F^2. All non-hydrogen atoms were refined with anisotropic thermal parameters. The hydrogen atoms were placed using a "riding model" and included in the refinement at calculated positions.

3. Results and discussion

3.1. Rh–Ti, Si heterometallic complexes

The chemistry of carboxylate [21–28], and in particular of salicylate complexes, has attracted a great deal of interest as a consequence of its importance in many areas such as catalysis or molecular architecture construction [29–35].

The titanium complex [TiCp*(Me)$_3$] reacts with salycilic acid in a 1:2 molar ratio to yield complex **1** (Scheme 1), which is isolated as a dark red solid. It is rather soluble in THF or toluene and less soluble in pentane or Et$_2$O.
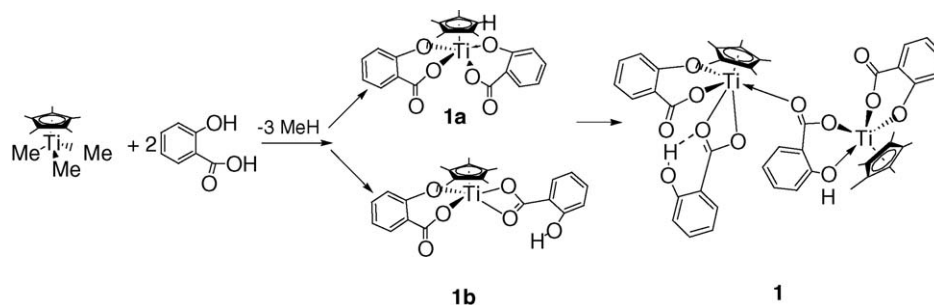
Scheme 1.

Complex **1** has been characterized by NMR and IR spectroscopy, as well as by elemental analysis and X-ray diffraction. The ^{1}H NMR spectrum shows two singlet signals at 1.87 and 2.11 ppm which are assigned to the Cp* ligand in each titanium centre along with several multiplet signals corresponding to the aromatic protons. The hydroxylic protons appear as broad absorptions at 10.19 and 12.80 ppm. The ^{13}C{^{1}H} NMR spectrum shows that all the four salycilate groups in the complex are in a different chemical environment. It can be obserseved 16 signals corresponding to the CH moieties and eight different peaks corresponding to the ipso carbon atoms. On the other hand, the IR spectrum, although not conclusively, indicates that the carboxylic moieties are coordinated to the metallic centers in different ways, monodentate, bidentate and as a bridge ligand. Given the multiple coordination modes of the salicylate ligand [36–38], we have carried out its characterization by X-ray diffraction methods in order to establish accurately the structure of this complex.

A diagram for the structure of **1** is shown in Fig. 1, and some selected bond distances and angles are summarized in the Appendix A.

The molecular structure shows it to be a dimetallic compound in which each one of the two metal centers, Ti1 and Ti2, are coordinated to one Cp* ligand and to two salicylate groups that exhibit different coordination modes. The Ti1 metal centre is bonded to both salicylate groups in a chelate fashion through one of the two oxygen atoms of the carboxylate moiety and the

aryloxide group. On the other hand, the Ti2 atom is bonded to one of the two salicylate groups in a similar fashion to that in Ti1, while the second one is bonded to the metal solely through the carboxylic moiety in a bidentate manner. Besides, Ti1 and Ti2 are bonded together through the carboxylate group of one of the salicylate ligands in Ti1 that is acting as bridging group. It is interesting to note that a single molecule displays all the coordination modes of carboxylic ligands, i.e., monodentate, bidentate and bridge.

It is possible that, in solution of toluene, complex **1** is present as mixture of the two isomers **1a** and **1b**. But in highly concentrated solutions, both isomers would assemble to yield the dark red crystals, which have been characterized (see Scheme 1).

It is also worth to point out that complex **1** still contains two hydroxyl groups. This characteristic makes it an interesting starting material in progressive molecular architectures construction.

Complex **1** reacts with [Rh(μ-OH)(COD]$_2$ to yield the hetero-bimetallic complex **2** (see Scheme 2) through a condensation reaction. It is scarcely soluble in most of the commonly used organic solvents.

Complex **2** has been characterized by some spectroscopic techniques as well as by elemental analysis. The NMR spectra show that it is a rather symmetric molecule. Both salicylate moieties are equivalent and give rise to four multiplet signal in the ^{1}H NMR spectrum. On the other hand, the Cp* ligand gives rise to a singlet signal at 2.12 ppm while the COD group shows a broad signal corresponding to the olefinic protons.

The rhodium derivative [Rh(μ-OH)(COD)]$_2$ reacts with (HOSiPh$_2$)$_2$O at room temperature in toluene to yield the corresponding rhodium siloxide **3** (Scheme 3). Complex **3** can be considered as a model of heterogeneous rhodium catalyst supported on silica. It has been characterized by some spectroscopic and analytical techniques as well as by X-ray diffraction methods. According to the NMR spectra, compound **3** is rather symmetric, the COD ligand as well as the siloxide ligand are
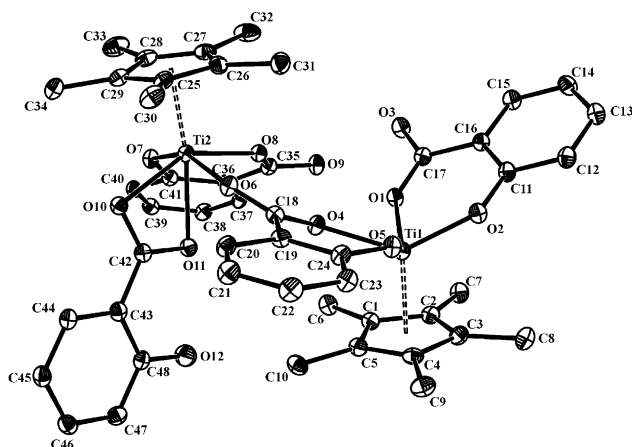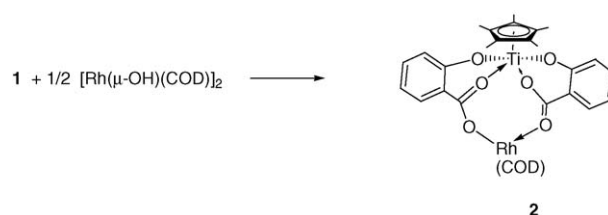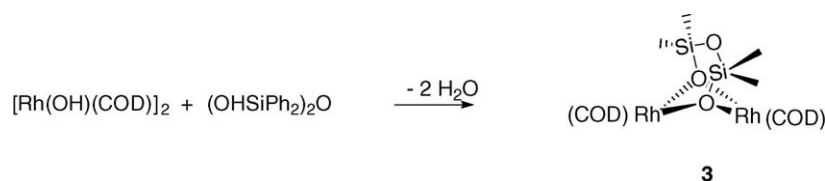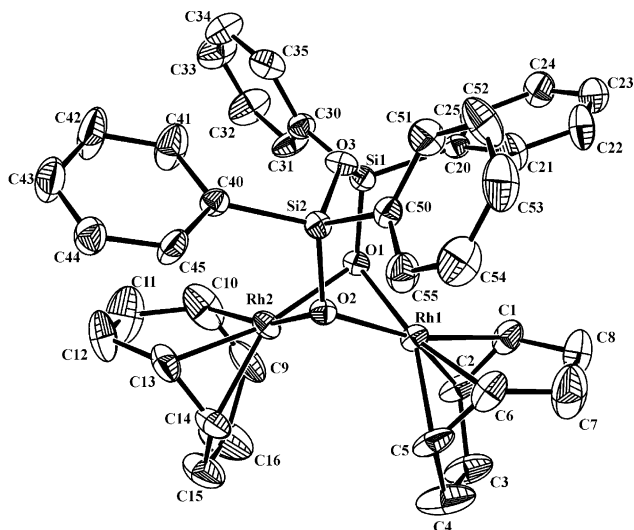

Fig. 1. An ORTEP representation of the structure of complex [Cp*Ti(sal)(salH)]$_2$ (**1**) showing the atom labelling scheme.

Scheme 2.

Scheme 3.

Fig. 2. An ORTEP representation of the structure of complex $[Rh(COD)]_2[\mu\text{-}(OSiPh_2)_2O]$ (**3**) showing the atom labelling scheme.

bisected by a mirror plane. On the other hand, all the phenyl groups are in an equivalent chemical environment.

An X-ray diffraction study was carried out in order to establish the molecular structure of complex **3**. Fig. 2 shows the ORTEP diagram of the molecule. Furthermore, the most important bond distances and angles are listed in the Appendix A.

The crystal structure shows that coordination around each rhodium atom is approximately square-planar. Two bridging oxygen atoms and a chelating cyclooctadiene are bonded to each metal atom. The Rh(1)–Rh(2) distance is rather short

(2.765(2) Å), and could be considered indicative of some metal–metal bonding interaction. Nevertheless, it could be also related to the small size of the bridging atom that forces the metal centres to be closer to each other [39]. The Rh–O bond lengths (Rh(1)–O(1), 2.121(5) and Rh(1)–O(2), 2.131(5) Å) are similar to those observed for other rhodium derivatives with bridging siloxide groups.

The Rh–C bond distances fall in the range 2.062(10)–2.114(8) Å, which are normal values for Rh(I) complexes containing COD ligands.

The Ti–Rh heterometallic derivative **2** reacts with an excess of carbon monoxide at room temperature under atmospheric pressure to yield the corresponding dicarbonyl complex **4** (see Scheme 4). Thus, the COD is easily replaced by carbon monoxide in complex **2** to give the orange heterometallic complex [Ti Cp*(sal)$_2$Rh(CO)$_2$] (**4**) with a good yield (61%). Complex **4** was isolated as a crystalline solid. It is highly insoluble in most common organic solvents and has been characterized by IR spectroscopy and by elemental analysis. The carbonyl derivative **4** can be synthesized as well by reaction of complex **1** and [Rh(acac)(CO)$_2$].

In an analogous way, the rhodium siloxide compound **3** reacts with CO at room temperature and atmospheric pressure to render the dicarbonyl derivative **5**. It has been isolated as a pale yellow complex and has been characterized by the normal spectroscopic techniques as well as by elemental analysis.

Complexes **4** and **5** can be envisaged as *gem*-Rh$^+$(CO)$_2$ species grafted on titania and silica respectively. The ν(CO) bands for both compounds **4** and **5** are located at 2084, 2009 and 2077, 2017 cm^{-1}, respectively. The pattern and the rel-
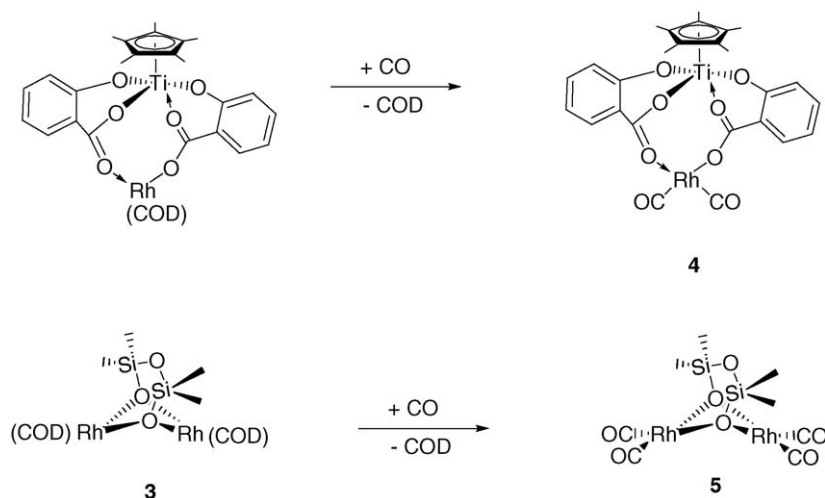
Scheme 4.

Table 1
Catalysts nomenclature

Catalyst	Rh source	Support	Rh (wt.%)	Pretreatment
Reference	$Rh(NO_3)_3$	γ-Al_2O_3	3	H_2/N_2, 533 K, 1 h
7	$[Rh(acac)(CO)_2]$	γ-Al_2O_3	3	H_2/CO
8	$[Rh(acac)(CO)_2]$	γ-Al_2O_3	3	H_2/N_2, 533K, 1 h
9	$[Rh(acac)(CO)_2]$	SiO_2	3	H_2/CO
10	$[Rh(acac)(CO)_2]$	SiO_2	3	H_2/N_2, 533K, 1 h
3	$[\{Rh(COD)\}_2\{\mu\text{-}OSiPh_2O\}]$	–		H_2/CO
6	$[Ti\ Cp^*\ (O_2Bz)2Rh(COD)]$	–		H_2/CO
2	$[Ti\ Cp^*(sal)_2Rh(COD)]$	–		H_2/CO
4	$[Ti\ Cp^*(sal)_2Rh(CO)_2]$	–		H_2/CO

ative intensity of absorptions is the expected for a *cis* dicarbonyl rhodium (I) complex [40,41]. They are comparable to the characteristic doublet of the ν_{sym}, ν_{asym} of the *gem*-dicarbonyl $Rh^+(CO)_2$ species prepared from different Rh precursors ($[Rh(\mu\text{-}Cl)(CO)_2]_2$, $[Rh(acac)(CO)_2]$, $[Rh(allyl)(CO)_2]$) on different oxide supports (SiO_2, Al_2O_3, TiO_2, zeolites) [42–48]. Also, the $Rh^0(CO)_2$ groups formed by adsorption of CO on Rh crystallites can react with the hydroxo groups of SiO_2 and Al_2O_3 to yield the $Rh^+(CO)_2$ species [49,50].

Compounds **3** and **5** can be considered as "a silica–silanol group" with an anchored transition metal complex [51–54]. The siloxanodiol can be compared with the vicinal diols present in the silica.

The catalytic activity of **2**, **3** and other closely related complexes $[Cp^*Ti(O_2Bz)Rh(COD)]$ (**6**) was studied in the CO hydrogenation reaction in order to determine if, despite the pretreatment conditions, the activity and selectivity reflects somehow the initial complex structure. The results are compared with those obtained using "standard" catalysts prepared from other rhodium precursors and oxide supports (silica, alumina). Catalyst nomenclature, rhodium precursors, supports and pretreatment conditions are summarized in Table 1.

The experimental reaction conditions were the following: 533 K, 2.03 MPa, 50 mL/min and $H_2/CO = 2$. In some cases, the catalysts were previously reduced in a H_2/N_2 flow at 533 K for 1 h. The reaction products were namely composed by hydrocarbons (C_1–C_{10}) and oxygenated compounds (1-alcohols).

3.2. Catalytic activity

Table 2 shows the results of CO hydrogenation with all the tested samples. First of all, it can be observed that all the Rh-based catalysts are active in the preparation of hydrocarbons and oxygenates from synthesis gas. However, the catalytic behaviour depends strongly on the catalyst precursor, pre-treatment and the nature of the oxide used as a support.

By comparing the catalysts named as **reference** and **8** ($Rh(NO_3)_3/\gamma$-Al_2O_3 versus $[Rh(acac)(CO)_2]/\gamma$-Al_2O_3), it can be seen that the appropriate election of the Rh precursor is very important. Thus, the catalyst made from rhodium nitrate precursor shows a higher CO conversion rate (about four times). Nevertheless, changes in reaction selectivity are not so clear. Both catalysts display about 50% selectivity to oxygenates.

With respect to the influence of the pre-treatment step, catalysts named as **7** and **8** should be compared. In this way, it is possible to investigate if the catalyst reduction in a H_2/N_2 flow affects its catalytic behaviour. From Table 2, it is clear that the CO conversion rate decreases after the hydrogen treatment. Simultaneously, oxygenates formation decreases and more hydrocarbons are formed. This could be tentatively explained assuming that some rhodium atoms have suffered sintering. As it has been published recently [55,56], oxygenates formation is favoured as the rhodium particle size diminishes. However, by comparing **9** and **10**, it can be observed that the activity remains constant after hydrogen treatment. This leads us to conclude that the rhodium particles are more stable against sintering where they are deposited over silica support instead of over alumina but the selectivity towards oxygenates increases.

The nature of the oxide used as a support also plays an important role. The effect of the supporting material can be observed by comparing samples **7** and **9** $[(Rh(acac)(CO)_2]/\gamma$-Al_2O_3 versus $[Rh(acac)(CO)_2]/SiO_2$). The catalytic activity is moderately affected. However, it can be observed that reaction selectivity is strongly influenced by the support. The alumina-supported sample shows higher selectivity to the oxygenated compounds. This is probably due to the interaction between the rhodium particles and the alumina support. The electrons of the rhodium atoms are attracted by the oxygen atoms of the support, leading to some partially positively charged $Rh^{\delta+}$ atoms [57]. Previous works have suggested that the typical Fischer–Tropsch catalysts

Table 2
Catalytic results for the CO hydrogenation over Rh-based catalysts

Catalyst	CO conv. (%)	mmol CO/h/ mmol Rh	C_1	C_2–C_4	C_{5+}	C_{oxyg}
Reference	7.3	26.8	31.7	12.0	7.3	49.1
7	4.2	15.4	35.1	8.8	2.3	53.5
8	2.1	7.7	23.6	28.5	1.9	46.0
9	2.4	11.1	9.0	50.0	17.2	23.8
10	2.4	11.1	17.4	22.2	4.8	55.6
3	8.1	25.0	27.5	43.1	4.0	25.4
6	13.7	41.4	23.8	27.4	5.4	43.4
2	56.0	195.9	21.6	17.1	5.4	56.0
4	8.8	161.1	21.6	14.6	4.8	59.0

Reaction conditions: 533 K, 2.03 MPa, $H_2/CO = 2$.

Table 3
Oxygenated products distribution

Cat.	mmolCO/h/mmol Rh	C_{oxyg}	C_2OH[a]	C_2O[b]	C_2OOMe[c]	C_2OOEt[d]	C_2OOH[e]	$C_{3+}O$[f]
Reference	26.8	49.1	20.8	7.4	4.8	13.5	0.3	2.3
7	15.4	53.5	17.2	7.0	6.8	14.2	6.7	1.6
8	7.7	46.0	17.9	0.0	8.8	13.6	3.9	1.8
9	11.1	23.8	6.5	14.7	0.0	0.0	0.0	2.6
10	11.1	55.6	19.1	35.4	0.0	0.0	0.0	0.9
3	25.0	25.4	18.0	3.8	0.0	0.0	0.0	3.6
6	41.4	43.4	23.6	0.0	4.6	9.6	2.4	3.2
2	195.9	56.0	24.9	1.4	3.8	18.4	5.6	1.9
4	161.1	59.0	24.8	7.7	7.3	13.1	4.3	1.8

Reaction conditions: 533 K, 2.03 MPa, $H_2/CO = 2$.

[a] C_2OH: ethanol.
[b] C_2O: acetaldehyde (+ methanol traces).
[c] C_2OOMe: methylacetate.
[d] C_2OOEt: ethyl acetate.
[e] C_2OOH: acetic acid.
[f] $C_{3+}O$.

can produce oxygenates when they are in δ+ oxidation states [58,59].

Several rhodium-based complexes have been also tested in the CO hydrogenation reaction (see catalysts named as **2**, **3**, **4** and **6**). The high activity of these complexes is not due to the formation of hot spots in the catalytic bed because the samples are highly diluted in SiC.

The thermogravimetric analysis of complexes **2** and **3** under H_2 shows an initial exothermic weight increase of 0.9 and 0.4% respectively, which is indicative of an uptake of H_2 or hydride formation. Compound **3** is very stable thermically, loosing the organic ligands between 483 and 573 K (48% yield). The theoretical yield for "Rh_2O_3Si" should be 37%, lower that the 41% obtained at 873 K. Compound **2** has a gradual weight loss between 120 and 873 K. The theoretical yield for "$RhTiO_2$" (27.4%) is also higher than the 31% yield at 873 K (Fig. 3).

The Rh–Ti bimetallic compounds (**2**, **4**, **6**) display a higher activity that the Rh–Si complex **3**. Moreover, the selectivity towards oxygenated products is much higher. Compounds **2** and **4**, containing salycilate ligands, are more active and selective than the alkoxide complex **6**. It is especially remarkable the per-

formance of complex **2**, which displays nor only the highest CO conversion, but also a high selectivity to the desired oxygenated compounds (Table 3). In this Table, it can be seen that most of the oxygenated compounds contain or come from oxygenates with two carbon atoms. Only trace amounts of methanol were detected. This observation shows up the ability of rhodium-based catalysts to insert CO into hydrocarbons chains, especially into CH_x units, which leads to C_2-oxygenates. The formation of two carbon atoms oxygenates has a great interest because these compounds are very important feedstocks for the chemical industry.

4. Conclusions

Although it is difficult to know the exact nature of the active centres in the reaction conditions, it can be seen that all complexes are more active than the conventional Rh-supported catalysts. The Ti–O–Rh bimetallic complexes exhibit a better performance that the Rh–O–Si complex being remarkable the effect of the salycilate ligand compare to the alkoxide.

5. Supplementary material

Crystallographic data for the structural analysis of 1 and 3 have been deposited with the Cambridge Crystallographic Data Centre, CCDC-284704 & 284705. Copies of this information may be obtained free of charge from The Director, CCDC, 12 Union Road, Cambridge CB2 1EZ, UK (fax: +44 1223 336033; E-mail: deposit@ccdc.cam.ac.uk or http://www.ccdc.cam.ac.uk).
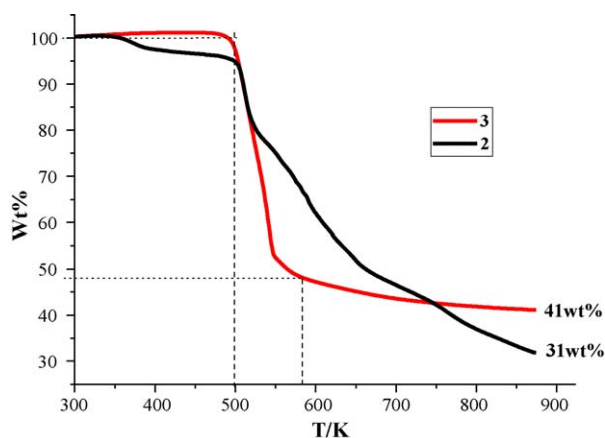

Fig. 3. TGA profiles of **2** and **3** under a flow of H_2, with a heating rate of $1\,K\,min^{-1}$.

Appendix A

Bond lengths [Å] for **1**: Ti(1)-[O(2)/1.897(2), O(5)/1.912(2), O(4)/2.015(2), O(1)/2.019(2)], Ti(2)-[O(7)/1.921(2), O(8)/1.998(2), O(6)/2.085(2), O(10)/2.095(2), O(11)/2.216(2)], C(1)-Ti(1)/2.379(4), Ti(2)-C42/2.521(4). Angles [°]: C(17)-O(1)-Ti(1)/135.7(2), C(11)-O(2)-Ti(1)/136.6(2), C(18)-O(4)-Ti(1)/134.4(2), C(24)-O(5)-Ti(1)/131.7(2), C(18)-O(6)-Ti(2)/142.9(2), C(41)-O(7)-Ti(2)/130.8(2), C(35)-O(8)-Ti(2)/132.2(2), C(42)-O(10)-Ti(2)/93.32(2), C(42)-O(11)-Ti(2)/88.2(2).

Bond lengths [Å] for **3**: Rh(1)-[Rh(2)/2.7646(14), O(1)/2.121(5), O(2)/2.131(5)]; Rh(2)-[O(2)/2.102(5), O(1)/2.133(4)]. Angles [°]: Si(1)-O(1)-Rh(1)/115.2(3), Si(1)-O(1)-Rh(2)/118.6(3), Si(2)-O(2)-Rh(2)/ 114.7(3), Si(1)-O(3)-Si(2)/130.1(3).

References

[1] S.J. Tauster, Acc. Chem. Res. 20 (1987) 389.
[2] J.F. Lambert, M. Che, J. Mol. Catal. A: Chem. 162 (2000) 5.
[3] J. Guzman, B.C. Gates, Dalton Trans. (2003) 3303.
[4] R. Fandos, C. Hernández, A. Otero, A. Rodríguez, M.J. Ruiz, P. Terreros, Chem. Eur. J. 9 (2003) 671.
[5] T.H. Fleisch, R.A. Sills, M.D. Briscoe, J. Nat. Gas Chem. 11 (2002) 1.
[6] J. Zhang, J. Chen, Y. Li, Y. Sun, J. Nat. Gas Chem. 11 (2002) 99.
[7] A.A. Adesina, Appl. Catal. A: Gen. 138 (1996) 345.
[8] P.M. Maitlis, J. Mol. Catal. A: Chem. 204–205 (2003) 54.
[9] P.M. Maitlis, J. Organomet. Chem. 689 (2004) 4366.
[10] M. Mena, M.A. Pellinghelli, P. Royo, R. Serrano, A. Tiripicchio, J. Chem. Soc., Chem. Commun. (1986) 1118.
[11] R. Usón, L.A. Oro, J.A. Cabeza, Inorg. Synth. 23 (1985) 126.
[12] D. Selent, M. Ramm, J. Organomet. Chem. 485 (1995) 135.
[13] M. Ojeda, M. López Granados, S. Rojas, P. Terreros, J.L.G. Fierro, J. Mol. Catal. A: Chem. 202 (2003) 179.
[14] M. Ojeda, M. López Granados, S. Rojas, P. Terreros, F.J. García-García, J.L.G. Fierro, Appl. Catal. A: Gen. 261 (2004) 47.
[15] G.M. Sheldrick, SADABS version 2.03, a Program for Empirical Absorption Correction; Universität Göttingen, 1997–2001.
[16] Bruker AXS SHELXTL version 6.10, Structure Determination Package, Bruker AXS 2000. Madison, WI.
[17] G.M. Sheldrick, SHELXS-97 Program for Structure Solution, Acta Crystallogr. Sect. A 46 (1990) 467.
[18] G.M. Sheldrick, SHELXL-97 Program for Crystal Structure Refinement; Universität Göttingen, 1997.
[19] A.C.T. North, D.C. Phillips, F.S. Mathews, Acta Crystallogr. Sect A 24 (1968) 351.
[20] A. Altomare, G. Cascarano, C. Giacovazzo, A. Guagliardi, J. Appl. Crystallogr. 26 (1993) 343.
[21] E. Mieczyńska, A.M. Trzeciak, J.J. Ziółkowski, T. Lis, J. Chem. Soc. Dalton Trans. (1995) 105.
[22] L. Carlton, M.P. Belciug, G. Pattrick, Polyhedron 11 (1992) 1501.
[23] E. Mieczyńska, A.M. Trzeciak, J.J. Ziółkowski, J. Mol. Catal. 80 (1993) 189.
[24] H. Werner, S. Poelsma, M.E. Schneider, B. Windmüller, D. Barth, Chem. Ber. 129 (1996) 647.
[25] U. Mörhring, M. Schäfer, F. Kukla, M. Schlaf, H. Werner, J. Mol. Catal. A: Chem. 99 (1995) 53.
[26] F. Kukla, H. Werner, Inorg. Chim. Acta 235 (1995) 253.
[27] H. Werner, M. Schäfer, O. Nürnberg, J. Wolf, Chem. Ber. 127 (1994) 27.
[28] F. Nicolò, G. Bruno, S. Lo Schiavo, M.S. Sinicropi, P. Piraino, Inorg. Chim. Acta 223 (1994) 145.
[29] V.G. Kessler, Chem. Commun. (1985) 1213.
[30] C.N.R. Rao, S. Natarajan, R. Vaidhyanathan, Angew. Chem. Int. Ed. 43 (2004) 1466.
[31] D.E. Edwards, M.F. Mahon, T.J. Paget, N.W. Summerhill, Transition Metal Chem. 26 (2001) 116.
[32] S.L. Castro, W.E. Streib, J.C. Huffmann, G. Christou, Chem. Commun. (1996) 2177.
[33] K. Gigant, A. Rammal, M. Henry, J. Am. Chem. Soc. 123 (2001) 11632.
[34] D.H. Gibson, Y. Ding, R.L. Miller, B.A. Sleadd, M.S. Mashuta, J.F. Richardson, Polyhedron 18 (1999) 1189.
[35] E. Mieczyńska, A.M. Trzeciak, J.J. Ziółkowski, T. Lis, Polyhedron 13 (1994) 655.
[36] M.G. Meirin, E.W. Neuse, M. Rhemtula, S. Schmitt, H.H. Brintzinger, Trans. Met. Chem. 13 (1988) 272.
[37] N.J. Brownless, D.A. Edwards, M.F. Mahon, Inorg. Chim. Acta 287 (1999) 89.
[38] G.B. Deacon, R.J. Phillips, Coord. Chem. Rev. 33 (1980) 227.
[39] A. Vizi-Orosz, R. Ugo, R. Psaro, A. Sironi, M. Moret, C. Zucchi, F. Ghelfi, G. Pályi, Inorg. Chem. 33 (1994) 4600.
[40] S. Rojas, J.L. García-Fierro, R. Fandos, A. Rodríguez, P. Terreros, J. Chem. Soc., Dalton Trans. (2001) 2316.
[41] M.A. Ciriano, F. Viguri, J.J. Pérez-Torrente, F.J. Lahoz, L.A. Oro, A. Tiripicchio, M. Tiripicchio-Camellini, J. Chem. Soc., Dalton Trans. (1989) 25.
[42] J. Evans, B.E. Hayden, M.A. Newton, Surf. Sci. 462 (2000) 169.
[43] B.E. Hayden, A. King, M.A. Newton, N. Yoshikawa, J. Mol. Catal. A: Chem. 167 (2001) 33.
[44] B.E. Hayden, A. King, M.A. Newton, Surf. Sci. 397 (1998) 306.
[45] J.M. Andersen, Platinum Met. Rev. 41 (1997) 132.
[46] J.A.M. Andersen, A.W. Currie, Chem. Commun. (1996) 1543.
[47] J. Evans, B. Hayden, F. Mosselmans, A. Murray, Surf. Sci. 301 (1994) 61.
[48] S.C.C. Chuang, G. Srinivas, A. Mukherjee, J. Catal. 139 (1993) 490, and references therein.
[49] P. Basu, D. Panayotov, J.T. Yates Jr., J. Am. Chem. Soc. 110 (1998) 2074.
[50] A.M. Thayer, T.M. Duncan, J. Phys. Chem. 93 (1989) 6763.
[51] B. Marciniec, H. Maciejewski, Coord. Chem. Rev. 223 (2001) 301, and references therein.
[52] K. Merz, S. Block, R. Schoenen, M. Driess, Dalton Trans. (2003) 3365.
[53] M. Nishiura, Z. Hou, Y. Wakatsuki, Organometallics 23 (2004) 1359.
[54] J. Jarupatrakorn, T.D. Tilley, Dalton Trans. (2004) 2808.
[55] M. Ojeda, S. Rojas, M. Boutonnet, F.J. Pérez-Alonso, F.J. García-García, J.L.G. Fierro, Appl. Catal. A: Gen. 274 (2004) 33.
[56] M. Ojeda, S. Rojas, F.J. García-García, M. López Granados, P. Terreros, J.L.G. Fierro, Catal. Commun. 5 (2004) 703.
[57] J. Raskó, J. Bontovics, Catal. Lett. 58 (1999) 27.
[58] H. Hayashi, L.Z. Chen, T. Tago, M. Kishida, K. Wakabayashi, Appl. Catal. A: Gen. 231 (2002) 81.
[59] J.P. Hindermann, G.J. Hutchings, A. Kinnenmann, Catal. Rev. Sci. Eng. 35 (1993) 1.